AN4016
Application note

2 kW PPA for ISM applications

Introduction

STMicoelectronics has recently introduced a new generation of high voltage DMOS products housed in STAC® air cavity packages and capable of delivering an output power of up to 1.2 kW for industrial, scientific, and medical applications such as 1.5 T and 3 T magnetic resonance imaging (MRI). This new air-cavity technology now enables lower thermal resistance, lower weight, and reduced cost compared to devices in ceramic packages.

In this application note we report on the design of a 2 kW-100 V, 123 MHz Class AB peak power amplifier (PPA) for 3 Tesla MRI applications. It almost doubles the output power of previous amplifiers using MOSFET transistors in standard ceramic packages. The design techniques and construction practices are described in enough detail to permit duplication of the amplifier. The devices used in this amplifier are two STAC4932B N-channel MOSFETs in a push-pull configuration capable of 1.2 kW each, under pulse conditions, and housed in the STAC244B, a bolt-down air cavity package.

The design goals for the amplifier are:

- Frequency: 123 MHz
- Supply voltage: 100 V
- Pulse conditions: 1 msec – 10%
- Output power: > 2 kW
- Gain: > 19 dB
- Efficiency: > 60%

Figure 1. STEVAL-IMR002V1

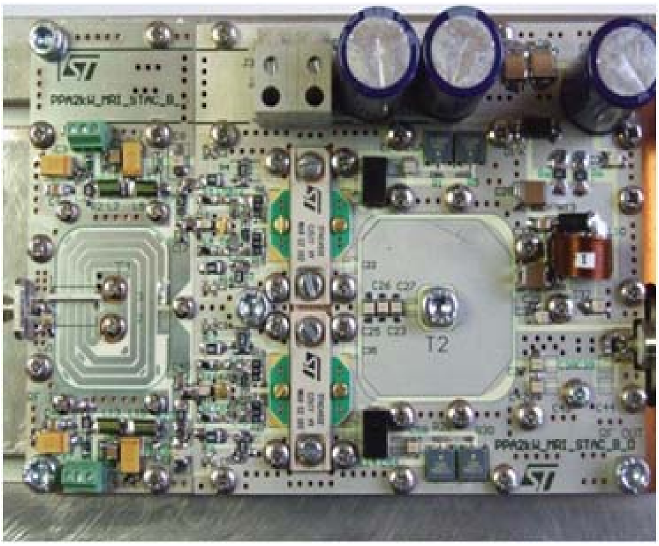

AM10219V1

Contents

1 Design choices 3

2 Circuit description 5

3 Layout, parts list, and design considerations 7

4 MRI board performance and application 14

5 Conclusion 15

6 References 15

7 Revision history 16

1 Design choices

The main objectives of the 2 kW power amplifier design are board compactness (100 x 150 mm), full SMT technology, and to avoid the use of ferromagnetic components and coaxial transmission line transformers.

In summary, see circuit diagram in *Figure 3*, the power amplifier uses double push-pull bolt-down devices, 2 x STAC4932B (see *Figure 2*) operate in Class AB. The two STACs are driven in push-pull through the transformer T1 together with two in-phase power splitters: this choice seems to be the best topology layout in terms of circuit size and mechanical compactness. Moreover, as the temperature coefficient of MOSFET channel resistance is positive, this makes a short-circuit possible in each pair of STAC4932B drains.

Figure 2. STAC244B bolt-down package

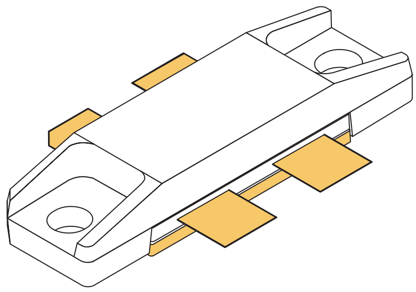

Figure 3. STEVAL-IMR002V1 circuit diagram

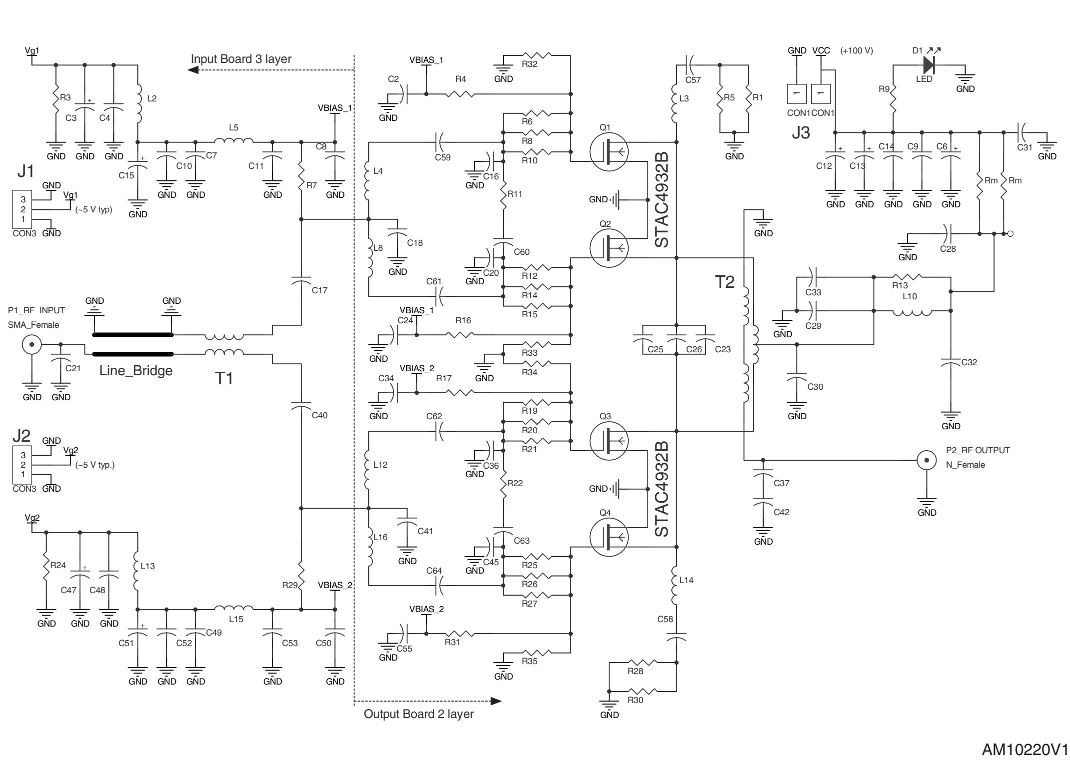

Therefore, a compact design can be realized: only one RF output matching network, with one impedance transformer T2, and an RF input matching network that supports the phase and amplitude signals on each of the two gates STAC4932B (electrical symmetry).

The schematic incorporates the necessary input / output biasing networks for proper feed biasing on the gates and drains.

Finally, planar microstrip technology was the main choice for the design of RF circuits: in particular, the design of transformers T1 and T2 is fully embedded into the substrate (PCB) itself as RF planar structures, and allows easy assembly of the design.

2 Circuit description

The Input RF network must be carefully designed respecting the correct electrical symmetry, because it is affected by driving high level signals (Pin ~ 20 W), and is made up of:

1. Balun transformer T1, λ / 4-25 Ohm transmission line type @ 123 MHz, needed to lower the 50 Ohm RF input impedance to 12.5 Ohm, and is realized in a stripline technique on a 2-layer substrate (Roger 4350B, with a thickness of 20 +20 mils: see *Figure 5*) and is fed by a suspended microstrip line ('line bridge' in *Figure 3*). Moreover, T1, being a quasi one-dimensional RF structure, can be mapped on the PCB without compromising the electrical symmetry. T1, finally, is loaded from R7 and R29 in order to dampen reflected waves from the gates and for stability purposes.
2. Two in-phase power splitters (L4, L8, C16, C18, C20) and (L12, L16, C36, C41, C45) simply decrease the impedance level (2 Ohm), and more importantly, allow the gates of each STAC4932 to be kept isolated.
3. RF decoupling filters, fed through the VG1 and VG2 connectors (*Figure 3*) need to bias each STAC4932B gate. They are essentially LC multi-section filters with capacitors of several technologies (tantalum, ceramic) to improve effective broadband RF isolation.

Independent voltage dividers act on the 4 gates (R4, R32, R16, R33, R17, R34, R31, R35) to assure broadband RF stability, while the lower value series resistors (R6, R8, R10, ...) need to dampen mismatching reflections on the gate impedance and then mitigate any asymmetries on the gate impedance value.

The output RF network acts on the DMOS drains, in order to achieve optimal impedance by means of the RF transformer T2, and also to properly feed high DC current filtered at Vd=100 V, through the output biasing network directly via the primary winding of T2.

The transformer T2 (ratio 4:1) is designed on the top/bottom layers (see *Figure 7*) using substrate Roger 4350B of 60 mils thickness in suspended broadside coupled strips and acts as a composite transmission line transformer in balanced to unbalanced mode. The RF output (type N-female connector) is directly connected to the winding output strip of T2 (see top view in *Figure 7*) through an air suspended microstrip-line (50 Ohm): in this way, the current (differential) generated on the primary winding strip (on the top layer) between the two STACs is moved from T2 versus unbalanced RF output by the ground of the plate copper carrier (see *Figure 8*) without further wave discontinuity, therefore avoiding losses and creating a reliable design to support very high RF output power.

The transformer T2 has been designed using commercially available SW (ADS, HFSS) and continues the refinement between electromagnetic and circuit simulation: T2, in fact, uses a lamped capacitor (C25, C26, C23 caps group on winding top strip, and C37, C42 caps group on the bottom side strip) to tune the proper impedance for DMOS drains.

In particular, the output biasing network (acts through the center tap of the winding top strip of T2) uses several multilayer ceramic capacitors, and also adds the following electrical functions:

1. Dampens voltage overshoot generated by each transient effected by pulsed RF modulation: that is the group L10, R13, C29, C30, C33.
2. Two test points can be inserted between two calibrated Rm resistors for current / voltage monitoring.
3. Lamp LED D1, for safety purposes.

Finally, the two bipole groups, consisting of L3-C37-R1/R5 and L14-C58-R28/R30, are inserted in the drain side of the amplifier and give more flexibility to the impedence, for example, it is used to improve low frequency stability, or to dominate harmonic impedance, or as broadband internal RF loads.

3 Layout, parts list, and design considerations

As mentioned previously (see *Figure 3*), the amplifier is built with separated input-output PCB cards:

a) The input PCB, as shown in *Figure 5*, integrates the RF balun transformer, T1, together with the RF decoupling networks.

b) The output PCB, see *Figure 7*, however, relates to the design of the RF transformer, T2, with the remaining biasing/filtering networks for the gates and drains of STAC4932B.

An image of the assembled board is shown in *Figure 1*, while *Table 1* gives the part list.

Figure 4, shows the final assembled board on the copper carrier and heatsink: board robustness is an important factor in order to ensure electrical stability to manage very high RF power.

The PCB cards are built in substrate Roger 4350B, in order to reduce dielectric losses through the Joule effect (50 to 100 W less when compared to FR4 @ 2 kW), and in particular to maintain thermal expansion compatibility with the copper carrier. Another aspect of this rigid thermoset laminate allows the creation of a PCB with very good surface finish, planarity and roughness, which are compatible with copper carrier surfaces that support it. In fact, a carefully finished PCB surface is recommended: HAL LF with tinned chemical deposition.

Moreover, accurate mounting procedures need to avoid bending/dirt that can compromise the planarity of PCB cards.

Figure 4. 2 kW MRI final assembled board

AM10221V1

Figure 5 and *Figure 7* show the input and output PCB cards, top and bottom-side. A mechanical drawing of the base-plate is shown in *Figure 8*: in particular, the two counterbores housing the transformers T1 and T2, are designed to control the unwanted parasitic impedance (leakage) to ground.

Figure 5. Input PCB, and top and bottom view

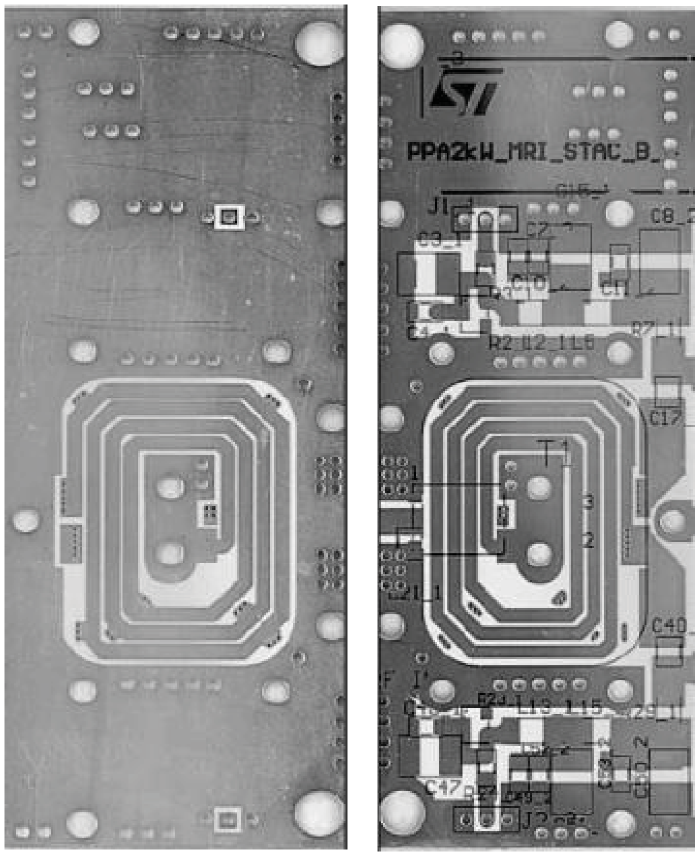

AM10222V1

The new package technology (STAC®) allows very low thermal impedance to be achieved, Rtjc = 0.075 K / W (with T = 1 msec pulsed RF/Duty = 10%), so that, in combination with a suitable heatsink (heatsink @ Rca <0.2 K / W max.), it permits the junction temperature to be lower than the rating (Tjmax = 200 degC): in fact, considering a 60% efficiency @ 2200 W, a DeltaTjc = 56 ° C, and DeltaTca <15 ° C, a Tj=95 ° C max. junction temperature can be expected.

The ability of STAC® to dissipate a high power pulse (see AN3232) allows the possibility to reduce board dimension and external heatsinks; so that, using the flangeless package STAC 244F (see *Figure 6*), you can design a new board with the same electrical characteristics but with a dimension target of 80 x 100 mm.

Figure 6. STAC244B

Figure 7. Output PCB, top and bottom view

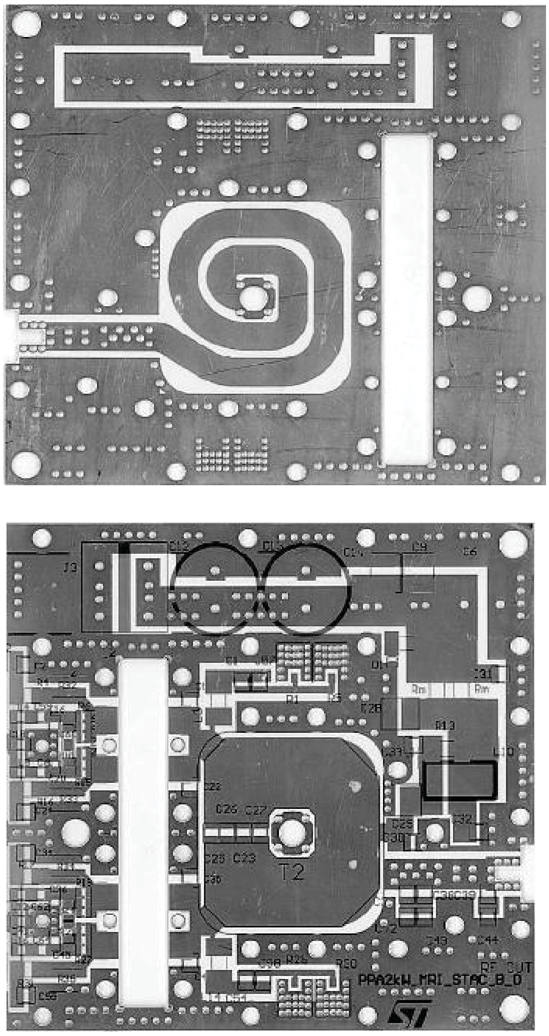

AM10223v1

Table 1. 2 kW MRI part list

Component ID	Value	Manufacturer	Part code
C12, C13, C6	1000 µF, 100 V	Panasonic	ECA2AM102
C10, C11, C52, C53	100 nF	Murata	GCM188R71E104KA57D
C28	4.7 µF, 100 V	TDK	CKG57NX7R1E226M
C29	15 µF, 100 V	Murata	KRM552R72A156M
C15, C51	10 µF, 35 V	KEMET	T494D106K035AT
C3,C47	100 µF, 20 V	KEMET	T491X107K020AT
C4, C7, C48, C49	22 µF, 25 V	Murata	GRM32ER61E226ME15
C18, C41	300 pF	ATC	ATC100B301FWN200XC
C16, C20, C36, C45	68 pF	ATC	ATC800A680JTN250X

Table 1. 2 kW MRI part list (continued)

Component ID	Value	Manufacturer	Part code
C30	1000 pF	ATC	ATC100B102FWN300XC
C57, C58	3.3 pF	ATC	ATC100B3R3BW1500XT
C8, C31, C32, C50	470 pF	ATC	ATC 100B 471FWN200XC
C2, C17, C24, C34, C40, C55, C59, C60, C61, C62, C63, C64	2000 pF	ATC	ATC 200A202KTN50C
C9, C14	1 µF, 100 V	AVX	22201C105KAT2A
C33	1 µF, 100 V	AVX	12101C105K4Z2A
C21	18 pF	ATC	ATC100B180FWN1500XT
C25	75 pF	ATC	ATC100B750FWN1500XC
C26, C23	100 pF	ATC	ATC100B101FWN1500XC
C37, C42	56 pF	ATC	ATC100B560FWN1500XC
L10	700 nH	Coilcraft	CP-K0376-A
L2, L5, L13, L15	82 nH	Coilcraft	1515SQ-82NJEB
L3, L14	110 nH	Coilcraft	132-10SMJ
L4, L8, L12, L16	5.4 nH	Coilcraft	0906-5JLB
R1, R5, R28, R30	50 Ω, 100 W	Anaren	C100N50Z4
R9	5600 Ω	Tyco Electronics	SMF25K6JT
R13	22 Ω	Tyco Electronics	SMW222RJT
R7, R29	100 Ω	Panasonic	ERJP14J101U
R11, R22	4.7 Ω	Vishay	4.7 Ohm -1206
R3, R24	43 Ω	Panasonic	ERJP14J430U
R32, R33, R34, R35	27 Ω	Panasonic	ERJP14J270U
R4, R16, R17, R31	20 Ω	Panasonic	ERJP14J200U
R6, R8, R10, R12, R14, R15, R19, R20, R21,R25,R26, R27	1 Ω	Phycomp	232271111108
Rm x 2	0.001 mΩ	Tyco Electronics	TL3A R001 1%
1P_J3	1 double pole	Wieland	25.700.0153.0
Spacer_J3	Spacer	Wieland	07.300.2753.0
3P_J1,J2	3 poles	PHOENIX CONTACT	1725669
P2	N_Female	Telegartner	J01021A1084
P1	SMA_Female	RADIALL	R124.510.000W
(Q1-Q2)/(Q3-Q4)	STAC4932B	STMicroelectronics	STAC4932B
D1	LED	Kingbright	KP-1608SURC

Table 2. Materials part list

Component	Description
Line bridge	Roger 4350B, three layers, 20+20 mils, 1 OZ Cu on top-mid-bottom layers, Finit. metal HAL LF; total Tk=1.2 mm max., top screen printing component, tin chemical surface deposition.
Board input	Roger 4350B, three layers, 20+20 mils, 1 OZ Cu on top-mid-bottom layers, Finit. metal HAL LF; total Tk=1.2 mm max., top screen printing comp., tin chemical surface deposition.
Fin fixing	Roger 4350B, two layers, Tk=60 mils, 1 OZ Cu on top- bottom layers, Finit. metal HAL LF; total Tk=1.6 mm max., top screen printing comp., tin chemical surface deposition.
Board output	Roger 4350B, two layers, Tk=60 mils, 1 OZ Cu on top-bottom layers, Finit. metal HAL LF; total Tk=1.6 mm max., top screen printing comp., tin chemical surface deposition.
Mechanical plate	PPAMRI_002-Rev B

Figure 8. Base-plate copper carrier

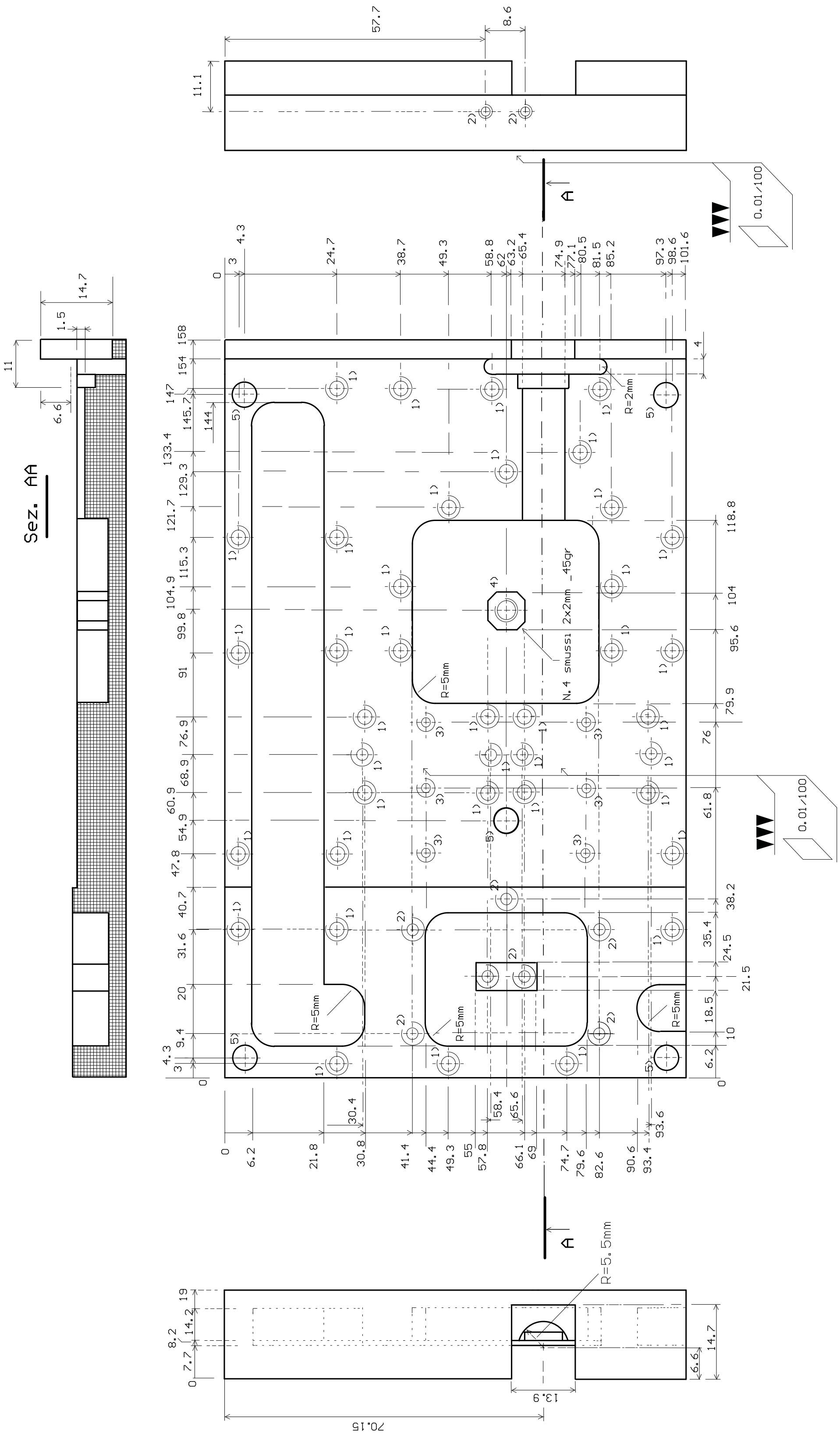

AM10224V2

4 MRI board performance and application

The power amplifier has been measured on two different RF scalar test benches: RF Power Lab. in STM Catania (Italy) and RF Power Lab. in STM Quakertown (USA): the measurements are in good agreement (+ / -0.15 dB max. error). The test includes a 2 kW/CW attenuator and a pulsed RF generator with high power amplifier driver to manage large signals at RF input (20 W min.) with good harmonic rejection (-30 dBc).

Figure 9. Gain and IRL frequency response

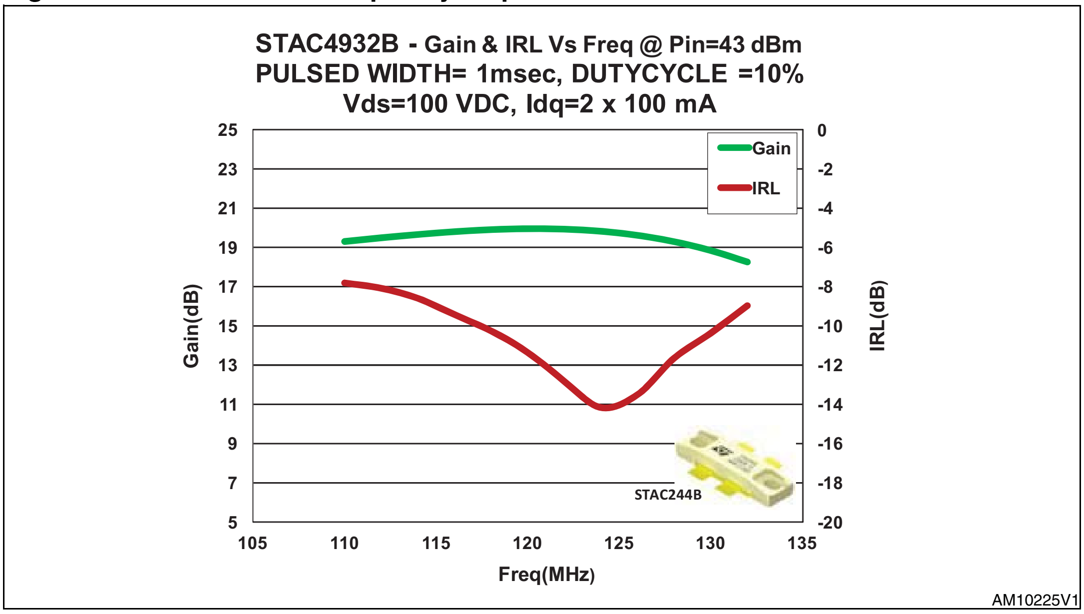

Figure 9 shows the large signal gain frequency response of the amplifier, as well as the input return loss, while *Figure 10* shows the gain compression curve and the drain efficiency curve Vs output power at 123 MHz (Idq = 200 mA and Vds = 100 V) and RF pulse width=1 msec, duty cycle=10%. The maximum efficiency is 60% @ 2.2 kW of output power.

Figure 10. Gain and drain efficiency vs. output power

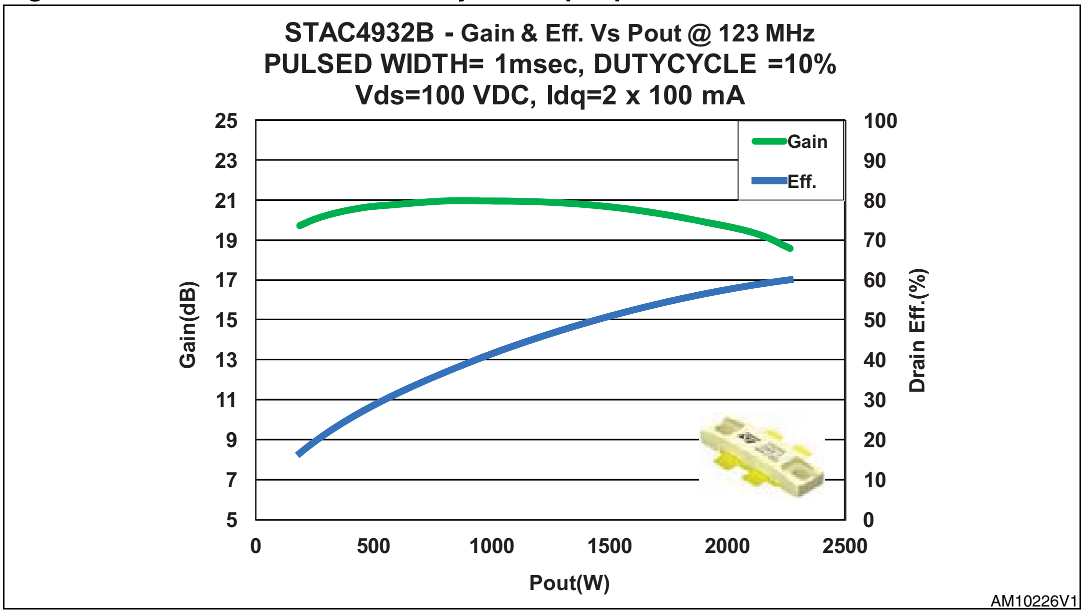

For IMS applications, two or more boards can be embedded to realize high power RF chains (4 kW or more): e.g., 10 kW RF power can be obtained by linking six RF basic units, properly using a Gysel power combiner, and integrated with the appropriate $\lambda / 4$ transmission lines to improve electrical stability, together with a control/monitoring card to support global safety.

5 Conclusion

A pulsed RF high power amplifier (> 2 kW) has been described as a guideline-design, oriented to new high voltage DMOS devices at Vd = 100 V: STAC4932B. In particular, the amplifier combines excellent high frequency response with an efficient use of DC power and allows a very compact design and robustness, in conjunction with SMT technology and joined to the fully planar microstrip design (RF transformers). This amplifier can be understood as the basic unit for high power RF chains to achieve very high power for an RF pulse generator in the RF systems for medical magnetic resonance imaging (3T-fMRI).

6 References

- RF and Microwave Power Amplifier Design, by Andrei Grebennikov - Mc Graw Hill, 2005.
- Essentials of RF and Microwave Grounding, by Eric Holzman - Artech House, 2006
- AN3232 application note.

7 Revision history

Table 3. Document revision history

Date	Revision	Changes
23-Dec-2011	1	Initial release.